

NASA Technical Memorandum 103687  
AIAA-91-0594

1N-02

1606

P 20

## Inflight Source Noise of an Advanced Full-Scale Single-Rotation Propeller

(NASA-TM-103687) INFLIGHT SOURCE NOISE OF  
AN ADVANCED FULL-SCALE SINGLE-ROTATION  
PROPELLER (NASA) 20 p CSCL 01A

N91-19045

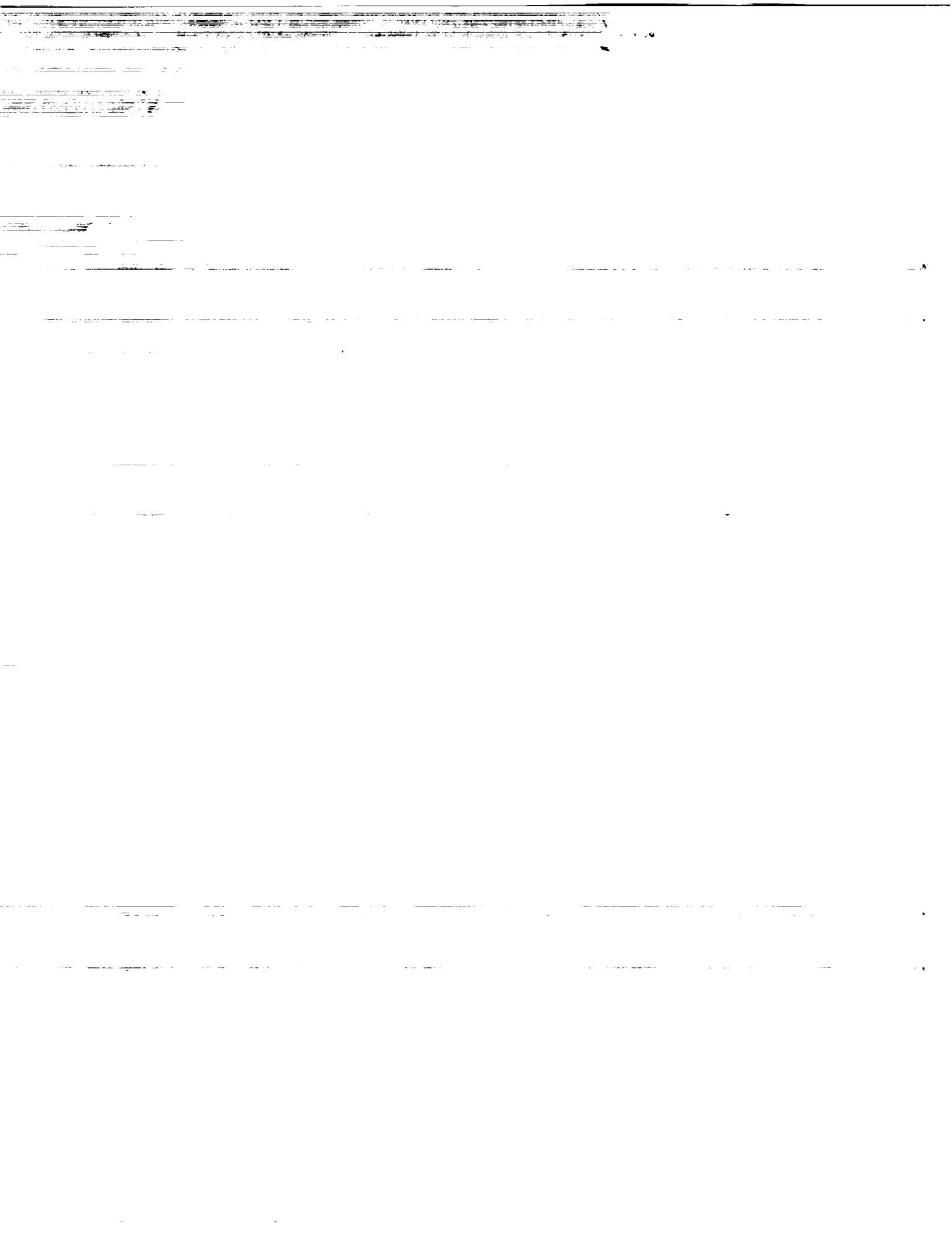
Unclas

G3/02 0001606

Richard P. Woodward and Irvin J. Loeffler  
*Lewis Research Center*  
*Cleveland, Ohio*

Prepared for the  
29th Aerospace Sciences Meeting  
sponsored by the American Institute of Aeronautics and Astronautics  
Reno, Nevada, January 7-10, 1991

**NASA**



# IN-FLIGHT SOURCE NOISE OF AN ADVANCED FULL-SCALE SINGLE-ROTATION PROPELLER

Richard P. Woodward and Irvin J. Loffler  
National Aeronautics and Space Administration  
Lewis Research Center  
Cleveland, Ohio 44135

## SUMMARY

E-5906

Flight tests to define the far field tone source at cruise conditions have been completed on the full-scale SR-7L advanced turboprop which was installed on the left wing of a Gulfstream II aircraft. This program, designated Propfan Test Assessment (PTA), involved aeroacoustic testing of the propeller over a range of test conditions. These measurements defined source levels for input into long-distance propagation models to predict en route noise. Inflight data were taken for 7 test cases. The sideline directivities measured by the Learjet showed expected maximum levels near  $105^\circ$  from the propeller upstream axis. However, azimuthal directivities based on the maximum observed sideline tone levels showed highest levels below the aircraft. An investigation of the effect of propeller tip speed (with other engine parameters, such as thrust, shaft power, flight speed, and altitude, held constant) showed that the tone level reduction associated with reductions in propeller tip speed is more significant in the horizontal plane than below the aircraft.

## INTRODUCTION

Modern high-speed propeller (advanced turboprop) aircraft are expected to operate on 50 to 60 percent less fuel than the 1980 vintage turbofan fleet while matching the flight speed and performance of these aircraft. They will consume 15 to 30 percent less fuel than advanced turbofan engines (ref. 1). However, the potential noise generated by such aircraft, which includes both in-flight cabin noise and community noise during takeoff and landing, requires investigation (ref. 2).

The NASA Lewis Research Center contracted with Lockheed Aircraft to modify a Gulfstream II aircraft as a flying testbed for an advanced single-rotation propeller and related propulsive hardware (refs. 3 and 4). This program, designated "PTA" (Propfan Test Assessment) involved extensive aeroacoustic testing of the installed propeller, which was mounted on the left wing of the Gulfstream II aircraft. (The Gulfstream's two aft-mounted turbojet engines were used for takeoff, landing, and auxiliary cruise power.) The test propeller, designated SR-7L, was manufactured for the project by the Hamilton Standard Division of United Technologies. The eight-blade propeller had a diameter of 2.74 M (9.0 ft). Design and performance results for the propeller and drive system may be found in references 5 to 7.

A prime objective of the PTA test was to map the propeller source noise directivity pattern of the SR-7L propeller under actual flight conditions. This test series was flown from the Lockheed-Georgia facility, and included both ground flyover noise measurements and inflight source noise mapping using the acoustically-instrumented NASA Learjet (refs. 8 to 11).

A "follow-on" test series with the PTA aircraft was conducted to obtain specialized data which was not acquired in the first test series. The scope of these follow-on tests included the ground and Learjet station-keeping noise measurements, to obtain a data base for en route noise, as well as propeller blade pressure, video

thermography, and structure-born noise measurements (ref. 12). These flights were flown out of El Paso, Texas with ground noise measurements (ref. 13) made at the White Sands, New Mexico, test range. Additional flights were made from the NASA Lewis Research Facility in Cleveland, Ohio. Figure 1 is a photograph of the PTA and Learjet aircraft flying in formation. The PTA aircraft/SR-7L propeller was operated at 7 test conditions that covered a range of propeller tip speeds and aircraft flight parameters. The source definition portion of the en route noise tests are the subject of this report. Reference 14 presents a comprehensive tabulation of the aeroacoustic results of this follow-on test program.

Extensive wind tunnel aeroacoustic tests of a 62.2 cm (24.5 in.) diameter model of the SR-7L (designated SR-7A) were made at the NASA Lewis Research Center prior to the full-scale flight tests. These tests explored noise directivities at cruise conditions (ref. 15) (0.7 Mach) and takeoff/approach conditions (ref. 16) (0.2 Mach). Results of these model propeller tests are not included herein.

This paper will present a synopsis of the full-scale SR-7L propeller acoustic results obtained by the Gulfstream and Learjet aircraft during these follow-on tests.

#### TEST PROCEDURE

The Gulfstream II aircraft was extensively modified by Lockheed-Georgia to accommodate the wing-mounted SR-7L propeller. As shown in the sketch of figure 2, these modifications included increasing the structural strength of the left wing and the addition of a counterbalance weight on the right wingtip. The Gulfstream aircraft carried instrumentation to monitor the aeroacoustic performance of the propeller as well as record the aircraft flight conditions.

The SR-7L propeller was designed for a 0.80 cruise Mach number at 10 688 M (35 000 ft) altitude (see Table I, and ref. 5). The 8-bladed propeller had a design tip speed of 244 M/sec (800 ft/sec). Figure 3 is a photograph of the SR-7L propeller installed on the Gulfstream wing. Figure 4 is a side view of the installed propeller.

#### Acoustic Instrumentation

Acoustic instrumentation on the Gulfstream included flush-mounted microphones on the aircraft fuselage and on an outboard microphone boom. Figure 5 shows the locations of these microphones relative to the SR-7L propeller. The fuselage microphones were located on a lateral line of closest propeller approach. The microphone boom was located outboard of the propeller diametrically opposite the line of fuselage microphones. The plane containing the propeller axis and the axes of the two microphone arrays is tilted approximately  $10^\circ$  from the horizontal. Both the fuselage microphones and boom microphones were at 1.12 propeller diameters from the propeller axis of rotation, or 0.62 diameters from the propeller tip. Thus, it is likely that data for these Gulfstream-mounted microphones include some near-field influences in the propeller noise measurements. The acoustic signals from the Gulfstream aircraft were recorded on analog tape aboard the aircraft for post-test analysis.

The NASA Lewis Learjet has been used for several propeller flight noise measurement tests (refs. 11, 17, and 18). The Learjet was instrumented with flush-mounted wingtip and nose side microphones for these earlier tests. Additional microphones were added to the Learjet nose top and cabin roof for the PTA station-

keeping tests to allow measurement of the propeller noise field below the aircraft in support of ground noise measurements and sound propagation theory validation. Two, essentially adjacent microphones were located at each measurement station, for a total of 12 microphones on the Learjet. Figure 6 is a photograph of the Learjet showing a wingtip microphone installation. The wingtip microphones were mounted on a plate (fig. 7) which replaced the navigation lights during the acoustic test flights. Figure 8 is a photograph of the Learjet showing the location of the nose side microphones. Figure 9 shows the locations of the Learjet microphones. The acoustic signals were monitored for data quality and recorded on magnetic tape aboard the aircraft for later analysis. The acoustic spectra of the Learjet engine noise were sufficiently different from those of the propeller to prevent significant data contamination.

#### Learjet Station-Keeping Positioning

Figure 10 is a sketch showing the designations for the sideline and azimuthal station-keeping locations used during formation flight. Two methods were used to fix the location of the Learjet relative to the SR-7L propeller (and Gulfstream aircraft), with the Learjet viewing the Gulfstream either visually or with a video camera and display. Sideline surveys at  $90^\circ$  and  $60^\circ$  azimuthal locations were flown optically, with the Learjet pilots maintaining visual contact with the Gulfstream. Surveys were initiated from behind the Gulfstream at the  $135^\circ$  or "G" location, and progressed forward as far as visual contact permitted. Aircraft separation for these cases was on the order of 61 M (200 ft). A 35 mm film camera mounted on a protractor device was used to verify the sideline angle. Photographs taken at each data point were later used with an image scaling technique to determine the actual source to microphone distances. The measuring station/microphone location geometry (fig. 9) of the Learjet were incorporated to determine the actual distance and measuring angle for each Learjet microphone.

Limited visibility of the Gulfstream from the Learjet resulted in a different positioning technique for the  $30^\circ$  and  $0^\circ$  azimuthal positions below the PTA aircraft. A wide-angle video camera was located such that it scanned upward through a viewing port in the Learjet cabin roof. Desired Gulfstream flight positions were then designated on viewing screens inside the Learjet. The Learjet pilots then flew the Learjet such that the Gulfstream was at the desired data location, as shown on a display template. The video flights were flown at typical sideline separations of about 154 M (500 ft). A third, "safety" aircraft was flown with the Gulfstream and Learjet for these "video" flights to ensure safe aircraft separation. The safety aircraft was flown sufficiently far away from the research aircraft to avoid signal contamination.

A shaft order signal from the SR-7L propeller was transmitted from the Gulfstream aircraft to the Learjet for inclusion in the analog data record. The plan was to use this signal for data enhancement to compensate for the increased aircraft separation distances associated with the  $30^\circ$  and  $0^\circ$  azimuthal locations. However, the signal enhancement techniques proved unsatisfactory due to separation distances, small relative aircraft movements, etc. Subsequently, the Learjet pilots determined that some of the  $30^\circ$  and  $0^\circ$  azimuthal location sidelines could be flown visually at the closer aircraft separation distances, with significantly greater data resolution. The video signal for the  $30^\circ$  and  $0^\circ$  azimuthal locations was recorded for later source-to-microphone distance calibrations using image scaling techniques.

## RESULTS AND DISCUSSION

### Propeller Aerodynamic Operating Conditions

Table II gives a description of the seven propeller test conditions, designated as cases 1 to 4, and 6 to 8. Case 5, which was at 610 M (2000 ft) altitude, was not part of the Gulfstream/Learjet follow-on test program due to safety concerns. Average test values are given in Table II for the measured propeller thrust, power coefficient, and shaft power. Values for the blade setting angle were not available during the follow-on test program, although the design setting angle (see Table I) was  $57.5^\circ$ . The SR-7L propeller setting angle was adjusted automatically in flight to compensate for power requirements. The unavailability of the blade setting angle value during these follow-on tests introduced an additional unknown in data comparisons between test cases. (Aerodynamic tests of the model, SR-7A, propeller indicated that a setting angle of  $60.1^\circ$  was required to achieve design performance at 0.80 Mach cruise conditions.)

Figure 11 is a propeller operating map of the power coefficient,  $C_p$ , versus advance ratio,  $J$ , for the target operating points. Cases 1, 7, and 8 provide a parametric study of the effect of propeller tip speed. The propeller was operating at essentially the same thrust and shaft power for these three cases. The power coefficient, which is inversely proportional to (rpm) (ref. 3) changes with tip speed. These three cases were flown at the design altitude of 10 688 M (35 000 ft). Case 6 performance came closest to the design point (from Table I). However, the tip speed for this case was 256 M/sec rather than the design 244 M/sec (800 ft/sec). Cases 2 and 3 explore performance at two flight speeds at 6096 M (20 000 ft) altitude; while case 4 was at 4267 M (14 000 ft) altitude.

### Acoustic Results

Acoustic measurements were made with flush-mounted microphones located on the Gulfstream fuselage and microphone boom, and on the Learjet aircraft. The acoustically-instrumented Learjet was flown along sidelines at a number of azimuthal locations for each propeller operating case. Data samples of approximately 1 minute duration were taken at designated angular locations along the sideline (see fig. 10). The acoustic data presented herein are for "as-measured" angular positions. Figure 12 shows the relationship between emission and as-measured angles for the four flight speeds. These differences can be significant. For example, at 0.70 Mach, a measured sideline angle of  $90^\circ$  corresponds to an emission angle of only  $46^\circ$ . This results in peak observed propeller tone levels occurring somewhat aft of the propeller plane. The sideline directivities for the model SR-7A propeller at cruise conditions showed similar shapes (ref. 15).

Figure 13 shows a representative spectrum for the SR-7L propeller. This spectrum is for the  $90^\circ$ L azimuthal angle ( $\phi = 90^\circ$ L) and  $118^\circ$  sideline angle with the propeller operating at case 1 conditions (see fig. 10 and Table II).

Adjustments to acoustic data for free-field results. - The acoustic data presented in this paper is adjusted to "free-field" conditions at a 152 M (500 ft) sideline distance relative to the propeller axis. These data adjustments are for spherical spreading ( $\Delta\text{dB} = 20 \log (D_1/D_2)$ ), and installation effects at the microphone measurement locations.

There is considerable debate as to the best procedure to correct for scattering, boundary layer refraction, and related flight effects at the microphone measuring station. Reference 19 presents theoretical and experimental data for free-field corrections for a microphone mounted on an infinite cylinder of various diameters. Results are presented for sound waves normal to the microphone surface and for a number of oblique impingement angles. Results in this reference are for "no-flow" conditions. While the correction procedures of reference 19 are relatively easy to apply, they do not properly account for airflow conditions, such as apply to the present results. References 20 to 23 present possible procedures to better account for airflow effects in correcting the microphone signals to free-field conditions. The importance of these corrections increase at sideline angles away from the propeller plane -- especially for upstream ( $\theta < 90^\circ$ ) measurements. It has been found that the procedure in reference 20, and by inference, references 21 and 22, does not quantitatively predict the boundary layer refraction at forward angles (ref. 24). However, it was felt that for a first approximation, the methods of reference 19, which is used in the following data presentations, gives reasonable results near the propeller plane, the region of highest tone level.

Sideline and azimuthal directivities. - Sideline and azimuthal tone directivities have been constructed from acoustic spectra measured by the Learjet at station-keeping locations. Broadband noise at the measuring microphone and distance attenuation of the propeller noise limited data acquisition at some sideline angles. This was especially true for higher-order tones at the  $30^\circ$  and  $0^\circ$  azimuthal angles, where video-positioning was used with a greater separation distance due to safety concerns.

Sideline directivities for the Gulfstream boom microphones are also shown on the  $90^\circ$ L sideline directivities to give some indication of distance effects (ie., near-field/far-field). The boom microphone which was located at 0.25 propeller diameters aft of the propeller plane (fig. 5) was inoperative throughout the follow-on test program. Again, the Gulfstream microphone boom was located, of necessity, at a relatively close 1.12 propeller diameters from the propeller axis of rotation. The following directivities are representative those taken during the follow-on tests. Additional directivity plots may be found in reference 14.

Figures 14 to 18 present tone directivities for the propeller operating at case 1 conditions. Case 1 (Table II) was flown at 10 688 M (35 000 ft) altitude with a propeller tangential tip speed of 244 M/sec (800 ft/sec). Figure 14 presents the fundamental tone sideline directivity at the  $90^\circ$ L azimuthal position ( $\phi = 90^\circ$ L), which is horizontal on the propeller side of the Gulfstream aircraft. A dashed line connects data points for the  $90^\circ$  and  $114^\circ$  Gulfstream boom microphones because of the inoperative  $103^\circ$  microphone. However, microphone boom data from the earlier PTA test series, during which the  $103^\circ$  was operative, showed that first and second-order tone levels for that microphone were similar to those for the  $90^\circ$  microphone.

There is a consistent difference between data taken by the Learjet nose microphones and that taken by the wingtip or cabin roof microphones. This difference has been noted in previous Learjet 13 flight noise studies (for example, see ref. 18); however, the reason for this difference remains unexplained. Typically, the wingtip and cabin roof tone level results are slightly higher than those for the nose microphones. A curve has been faired through the data from either the Learjet nose or wingtip and cabin roof measuring stations for the sideline directivities presented herein.

The sideline directivities taken by the Learjet in figure 14 show a maximum tone level at a sideline angle of about  $105^\circ$ , which is as expected from similar model data at cruise conditions (ref. 15). The unavailability of the Gulfstream boom microphone which was located 0.25 propeller diameters aft of the propeller plane ( $103^\circ$  sideline angle) was unfortunate since data from that microphone should be near the maximum sideline tone level. A dashed line is used for the microphone boom directivities to denote the level uncertainty due to the missing middle microphone. It is possible that data for the aft two boom microphones (located at sideline angles of  $114^\circ$  and  $132^\circ$ ) might be affected by proximity to the aircraft structure.

The Learjet took data along a number of sidelines, primarily to define the far-field data field of the SR-7L propeller for use as input to long-distance propagation models used to predict en route flyover noise. In particular, the relatively close far-field data taken by the Learjet may be used in conjunction with corresponding ground noise measurements to validate models for acoustic propagation over long distances. (Atmospheric measurements were taken concurrently with the ground flyover data acquisition for input in the acoustic propagation theory (ref. 13). Figure 15 shows the fundamental tone sideline directivities directly below the propeller (the  $\phi = 0^\circ$  azimuthal position). Data are from the Learjet nose and cabin roof microphones. Again, curves were faired through points from each of the microphone measuring locations. These faired curves are estimates of the directivity and have some degree of uncertainty. For example, curves faired through the sideline data of figure 15 have a potential error of about 2 dB. Maximum tone levels again occurred at about  $105^\circ$  sideline angle, and maximum tone level results for the cabin roof microphones were about 4 dB higher than those for the nose microphones.

Figure 16 shows the  $90^\circ$ L sideline tone directivities for the second harmonic propeller tone. Results for the Learjet nose and wingtip microphones are in much better agreement than was observed for the fundamental tone directivities of figure 14, suggesting that the aforementioned measurement differences may be related to tone frequency (and frequency-related sound reflections, etc.). However, this tone frequency argument for the measuring station difference has limited validity. For example, fundamental sideline directivities at the  $90^\circ$ L position for cases 4, 6, and 7 show reasonably good agreement between data for the two Learjet measuring locations, while corresponding second harmonic data for case 8 shows nose/wingtip differences similar to those noted for case 1.

Figures 17 and 18 show the azimuthal directivity of the maximum first and second-order sideline tone level observed by the Learjet. Again, results are shown for the nose and the wingtip/cabin roof microphones. The wingtip microphone results were used for the  $90^\circ$  and  $60^\circ$  data, while the cabin roof (and nose top) microphones were used at  $30^\circ$  and  $0^\circ$ .

The fundamental azimuthal directivities of figure 17 show that the level difference between the two Learjet measuring stations is consistent and appears at all measured azimuthal locations. There is generally a higher tone level toward the  $0^\circ$  azimuthal location relative to the  $90^\circ$ L location. This circumferential variation is associated with propeller operation at non-zero axis angle-of-attack. Propeller operation at positive angles of attack would be expected to yield an azimuthal directivity with highest levels below the propeller (and lowest levels above the propeller). Takeoff (0.20 Mach) windtunnel noise measurements of the model SR-7A propeller (ref. 16) showed the fundamental tone level below the propeller to increase nearly 1 dB for each degree of positive angle of attack. The propeller operated at



approximately 3° positive angle-of-attack at case 1 conditions, so the circumferential variation observed in figure 17 (at cruise conditions) is expected.

The nacelle tilt angle was fixed at -1.0° through these follow-on flight tests. The upwash angle at the propfan estimated from panel method calculations (ref. 10) was about 1.0°, effectively cancelling the nacelle tilt angle such that the measured aircraft angle-of-attack was close to the actual propeller inflow angle. Reference 25 compares SPL tone levels measured at the PTA aircraft boom and fuselage microphones with tone level predictions for several propeller angles-of-attack, again showing through both theory and data that there is a region of higher noise below (and also on the microphone boom side of the aircraft) for propeller operation at positive angles-of-attack.

Figure 18 shows the case 1 azimuthal directivities for the second harmonic propeller tone. These results are similar in nature to those for the fundamental tone of figure 17, showing a slightly higher level below the aircraft.

Figure 19 shows the case 2 azimuthal directivity for the fundamental tone as measured by the Learjet microphones. These data are reported because sideline angles from 90°L to 90°R are represented. Of particular interest in this figure are the sharply lower tone levels near the 90°R azimuthal location, where Gulfstream fuselage blocking of the propeller sound path becomes significant.

Propeller tip speed effects. - Propeller test cases 1, 7, and 8 afforded the opportunity to explore the acoustic field of the full-scale SR-7L propeller at different tip speeds. Flight conditions remained essentially unchanged for these three test cases, including propeller operation in terms of thrust and shaft power (Table II). These tests were conducted at 10 688 M (35 000 ft) altitude at 0.70 Mach.

Reference 26 summarizes the Gutin analysis of the acoustic effects of varying propeller tip speed and number of blades (with other parameters, such as thrust and power held constant). The estimate of the strength of the "mth" harmonic for a propeller is given as:

$$mnJ_{mn} (0.8M_t mn \sin \theta)$$

where  $m$  is the order of the harmonic,  $n$  is the number of blades,  $M_t$  is the blade tip rotational Mach number,  $\theta$  is the sideline angle relative to the upstream axis of rotation, and  $J_p(x)$  is a Bessel function of the first kind of order  $p$  and argument  $x$ . This expression of the harmonic strength may be used to give a rough estimate of the expected tone level reduction with reduced tip speed. Application of this expression reasonably predicts changes in maximum tone level associated with blade tip speed changes at low flight speeds where blade loading noise dominates (ref. 27). However, there is some question as to the validity of the Gutin expression when the blade helical tip mach number approaches unity and transonic aerodynamics influence blade loading. Blade thickness noise, which is not accounted for by Gutin, also becomes more significant at high helical tip Mach numbers. Reference 15 showed that tone noise for the model SR-7A propeller at cruise conditions ( $M = 0.7$ ) was still controlled by loading noise near the propeller plane (maximum noise) location. (Thickness noise appeared to dominate the model propeller upstream tone directivity above  $M = 0.7$ ). Hence, the Gutin expression for tone level as a function of propeller tip speed is, at best, a qualitative indicator of tone level behavior for the SR-7L propeller at 0.7 Mach cruise conditions.

Applying this expression to cases 7, and 8 with respect to case 1 gives an estimated first-order tone reduction of 7.2 dB for case 7 and 11.3 dB for case 8, respectively. Somewhat higher tone reductions of 11.9 and 20.0 dB, respectively, are predicted for the second-order propeller tone.

Figure 20 shows fundamental tone directivities at the 90°L sideline as measured by the Learjet microphones. Figure 20(a) shows results for the nose microphones, while results for the wingtip microphones are shown in figure 20(b). The data curves in figure 20 and subsequent comparison figures were faired through the individual data points as described in the discussion of figure 14. These sideline results show a tone level reduction associated with reduced propeller tip speed. Additionally there appears to be a shifting of the maximum tone levels toward sideline angles with reduced propeller tip speed.

The effect of propeller tip speed reduction on the maximum tone level is significantly less below the propeller ( $\phi = 0^\circ$ ) as shown in figure 21. Also, the shape of the directivity curves (ie., angular location of maximum tone level) showed little change for the three test cases (except for the case 8 results for the cabin roof microphones in figure 21(b), which showed a forward shift in directivity)

Second-order tone level results measured by the Learjet were only retrievable from the data for cases 1 and 8 at the 90°L azimuthal location. Figure 22 shows the second harmonic sideline directivities for these two cases. Again, there is a significant tone level reduction associated with reduced propeller tip speed.

The azimuthal directivities of the maximum sideline tone levels measured by the Learjet for cases 1, 7, and 8 are presented in figure 23. Results are similar for the Learjet nose microphone data (figure 23(a)) and the wingtip microphones (figure 23(b)), showing that the greatest benefits of reduced propeller tip speed appear to occur toward the 90°L azimuthal position, with minimal benefits below the aircraft. Note that the propeller axis angle-of-attack was constant at +3° for these three cases.

Figure 24 summarizes the effect of reduced propeller tip speed for the first two propeller tone orders. Results are shown for the maximum tone levels observed along the 90°L and 0° sidelines by the Learjet nose, wingtip, and cabin roof microphones, and for the Gulfstream boom microphones. Predicted tone reductions with reduced propeller tip speed using the approach of reference 25 are also shown on this figure. Again, the Gutin prediction of this reference is more applicable to lower axial Mach numbers, where loading noise is the primary tone generation mechanism. Observed tone level reductions for cases 7 and 8 approach, but do not reach, predicted values for the fundamental tone (figure 24(a)) at the 90°L azimuthal position. Results for the microphone boom, which was located slightly below the 900L sideline are similar to those measured by the Learjet. Again, little tone level reduction was observed below the aircraft. Level reductions with reduced tip speed for the second-order tone at the 90°L azimuthal position (figure 24 (b)) were about the same as for the fundamental tone, although the predicted decreases in tone level were significantly greater.

#### CONCLUDING REMARKS

Flight tests to define the far field tone source have been completed on the full-scale SR-7L advanced turboprop which was installed on the left wing of a Gulfstream II aircraft. This program, designated Propfan Test Assessment (PTA),

involved aeroacoustic testing of the propeller over a range of test conditions. These measurements defined source levels for input into long-distance propagation models to predict en route noise. In-flight data were taken for 7 test cases. Three of these cases allowed an investigation of the effect of propeller tip speed 6ulf5X on tone noise at 10 688 M (35 000 ft) and 0.70 Mach flight conditions.

The sideline directivities measured by the Learjet showed expected maximum levels near 105° from the propeller upstream axis. However, azimuthal directivities based on the maximum observed sideline tone levels showed highest levels below the aircraft. An investigation of the effect of propeller tip speed (with other engine parameters, such as thrust, shaft power, flight speed, and altitude, held constant) showed that the tone level reduction associated with reductions in propeller tip speed is more significant in the horizontal plane than below the aircraft.

#### REFERENCES

1. Whitlow, J.B. Jr., and Sievers, G.K.: Fuel Savings Potential of the NASA Advanced Turboprop Program, NASA TM-83736, 1984.
2. Groeneweg, J.F., and Bober, L.J.: NASA Advanced Propeller Research, NASA TM-101361, 1988.
3. Poland, D.T., Bartel, H.W., and Brown, P.C.: PTA Flight Test Overview, AIAA Paper 88-2803, 1988.
4. Little, B.H., Poland, D.T., Bartel, H.W., and Withers, C.C.: Propfan Test Assessment (PTA) Final Project Report, NASA CR-185138, 1989.
5. DeGeorge, C.L.: Large-Scale Advanced Prop-fan (LAP), NASA CR-I82112, 1989.
6. Withers, C.C., and Bartel, H.W.: Static Tests of the PTA Propulsion System, AIAA-87-1728, 1987.
7. O'Rourke, D.M.: Propfan Test Assessment Propfan Propulsion System Static Report, NASA CR-179613, 1987.
8. Bartel, H., and Swift, G.: Near-Field Acoustic Characteristics of a Single-Rotor Propfan, AIAA-89-I055, 1989.
9. Reddy, N., Bartel, H., and Salikuddin, M.: Installed Propfan (SR-7L) Far-Field Noise Characteristics, AIAA-89-1056, 1989.
10. Little, B.H., Bartel, H.N., Reddy, N.N., Swift, G., and Withers, C.: Propfan Test Assessment (PTA) Flight Test Report, NASACR-182278, 1989.
11. Woodward, R.P., and Loeffler, I.J.: Cruise Noise of an Advanced Single-Rotation Propeller Measured from an Adjacent Aircraft, Internoise 1989 proceedings, pp. 243-248, 1989.
12. Unruh, J.: Structure-Born Noise Transimission in the Propfan Test Assessment Aircraft (PTA), AIAA-90-3966, 1990.

13. Wilshire, W.L., and Garber, D.P.: En Route Noise Test Preliminary Results, Internoise 1989 Proceedings, pp. 309-312, 1989.
14. Woodward, R.P., and Loeffler, I.J.: In-Flight Near and Far Field Acoustic Data Measured on the Propfan Test Assessment (PTA) Testbed and with an Adjacent Aircraft, NASA TM-103719, 1991.
15. Dittmar, J.H., and Stang, D.B.: Cruise Noise of the 2/9th Scale Model of the Large-Scale Advanced Propfan (LAP) Propeller, SR-7A, NASA TM-100175, 1987.
16. Woodward, R.P.: Measured Noise of a Scale Model High Speed Propeller at Simulated Takeoff/Approach Conditions, AIAA-87-0526, 1987.
17. Balombin, J.R., and Loeffler, I.J.: Farfield Inflight Measurements of High-Speed Turboprop Noise, AIAA-83-0745, 1983.
18. Woodward, R.P., Loeffler, I.J., and Dittmar, J.H.: Measured Far-Field Flight Noise of a Counterrotation Turboprop at Cruise Conditions, NASA TM-101383, 1989.
19. Wiener, F.M., "Sound Diffraction by Rigid Spheres and Circular Cylinders, J. Acoustic Society of America, Vol. 19, No. 3, May, 1947, p. 444.
20. Hanson, D.B., and Magliozzi, B.: Propagation of Propeller Tone Noise Through a Fuselage Boundary Layer, J. Aircraft, Vol. 22, No. 1, Jan. 1985, pp. 63-70.
21. McAnich, G.L., and Rawls, J.W., Jr.: Effects of Boundary Layer Refraction and Fuselage Scattering on Fuselage Surface Noise from Advanced Turboprop Propellers, AIAA-84-0249, 1984.
22. McAnich, G. L.: Effects of Velocity Profile on Boundary Layer Shielding, AIAA-87-2678, 1987.
23. Lu, H.Y.: Fuselage Boundary-Layer Effects on Sound Propagation and Scattering," AIAA Journal, Vol 28, No. 7, July, 1990, pp. 1180-1186.
24. Dittmar, J.H., and Krejsa, E.A.: Predicted and Measured Boundary Layer Refraction for Advanced Turboprop Propeller Noise, NASA TM-102365, 1990.
25. Nallasamy, M, Envia, E., Clark, B.J., and Groeneweg, J.F.: Near-Field Noise of a Single Rotation Propfan at an Angle of Attack, AIAA-90-3953, 1990
26. Richards, E.J., and Mead, D.J.: Noise and Acoustic Fatigue in Aeronautics, John Wiley & Sons, New York, 1968, p. 189.
27. Woodward, R.P., and Hughes, C.E.: Aeroacoustic Effects of Reduced Aft Tip Speed at Constant Thrust for a Model Counterrotation Turboprop at Takeoff Conditions," AIAA-90-3933, 1990.

TABLE I. - SR-7L PROPELLER DESIGN PARAMETERS

[Cruise conditions.]

Diameter, M (ft)	2.74 (9.0)
Number of blades	8
Mach number	0.80
Altitude, M (ft)	10 668 (35 000)
Tip speed, M/sec (ft/sec)	244 (800)
Rotational speed, rev/min	1698
Blade setting angle, 3/4 span, deg <sup>a</sup>	57.57
Advance ratio	3.06
Power coefficient	1.45
Power loading, kW/m <sup>2</sup> (hp/ft <sup>2</sup> )	257 (32.0)
Excitation factor	4.5
Power, kW (hp)	1934 (2592)
Thrust, N (lbf)	6490 (1459)

<sup>a</sup>Aerodynamic tests of the reduced-diameter SR-7A propeller showed that design conditions were met with a blade setting angle of 60.1°

TABLE II. - SR-7L PROPELLER TEST CONDITIONS

Case number	Mach	Altitude		Propeller tangential tip-speed		Thrust		Power coefficient, C <sub>p</sub>	Shaft power		Percent full power
		M	ft			N	lbf		kW	hp	
				M/sec	ft/sec						
1	0.70	10 668	35 000	244	800	6 230	1400	1.35	1790	2400	90
2	0.70	6 096	20 000	↓	↓	9 920	2230	1.43	3210	4300	↓
3	0.50	6 096	20 000	↓	↓	12 721	2860	1.27	2820	3780	↓
4	0.59	4 267	14 000	↓	↓	13 790	3100	1.15	3130	4200	↓
6	0.77	10 668	35 000	256	840	6 630	1490	1.47	2090	2800	100
7	0.70	10 668	35 000	213	700	6 230	1400	1.98	1810	2430	90
8	0.70	10 688	35 000	189	620	6 010	1350	2.46	1810	2420	90

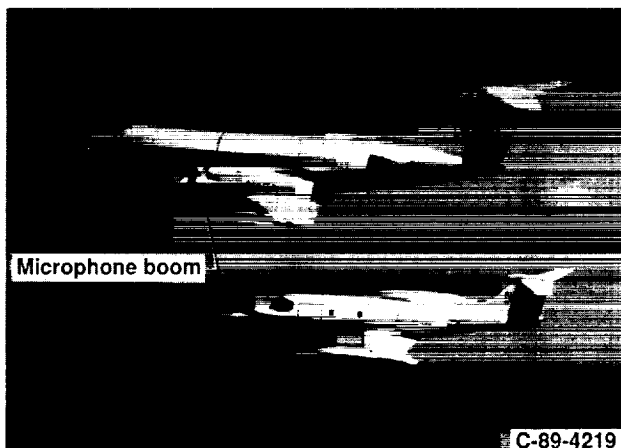


Figure 1.—In-flight photograph of PTA and Learjet aircraft.

ORIGINAL PAGE  
BLACK AND WHITE PHOTOGRAPH

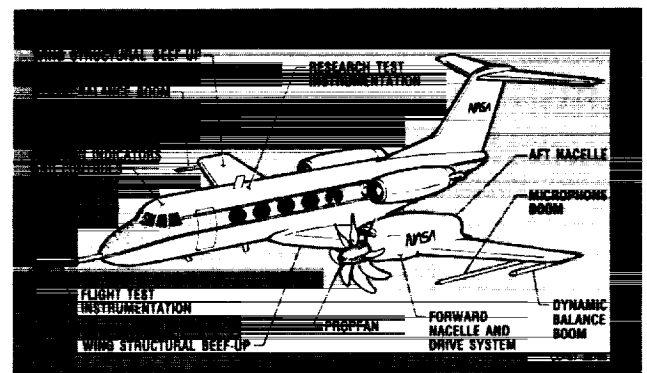


Figure 2.—Modifications to Gulfstream II aircraft to PTA configuration.

ORIGINAL PAGE IS  
OF POOR QUALITY

ORIGINAL PAGE  
BLACK AND WHITE PHOTOGRAPH



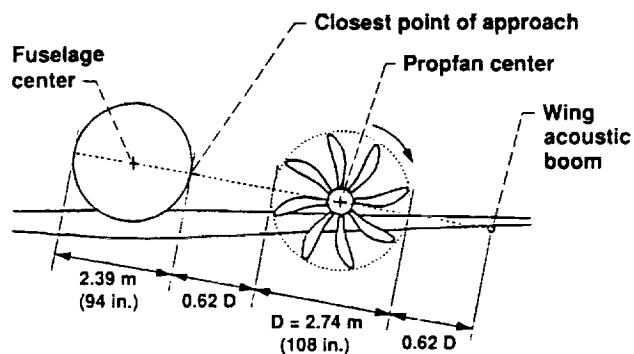
C-89-7238

Figure 3.—SR-7L propeller installed on Gulfstream II aircraft.

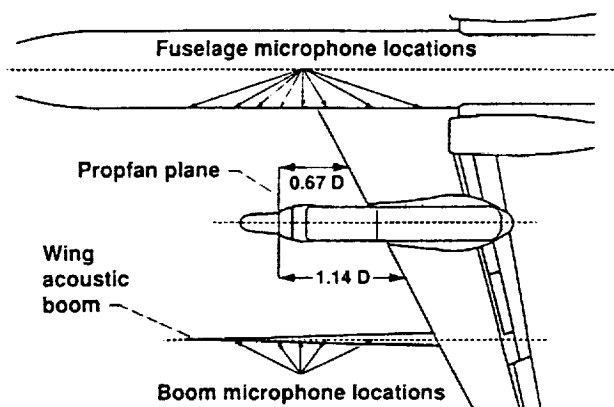


C-89-7236

Figure 4.—Side view of SR-7L propeller.



(a)



(b)

	Forward locations	Propfan plane	Aft locations
Axial distance from propfan plane, X/D	1.00 -0.50 -0.25	0.00	0.25 0.50 1.00 1.50
Boom microphones	•	•	• • •
Fuselage microphones	• • •	•	• • • •

Figure 5.—PTA acoustic instrumentation.

ORIGINAL PAGE IS  
OF POOR QUALITY

ORIGINAL PAGE  
BLACK AND WHITE PHOTOGRAPH

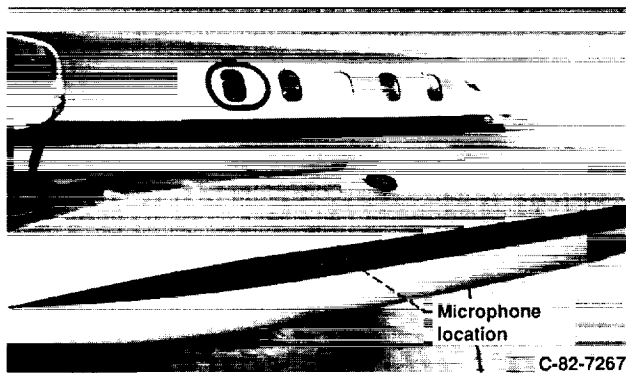


Figure 6.—Learjet wingtip microphone installation.

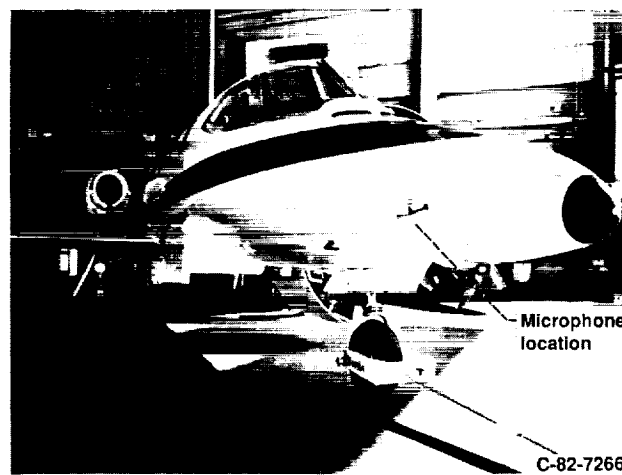


Figure 8.—Learjet nose microphone installation.

ORIGINAL PAGE IS  
OF POOR QUALITY

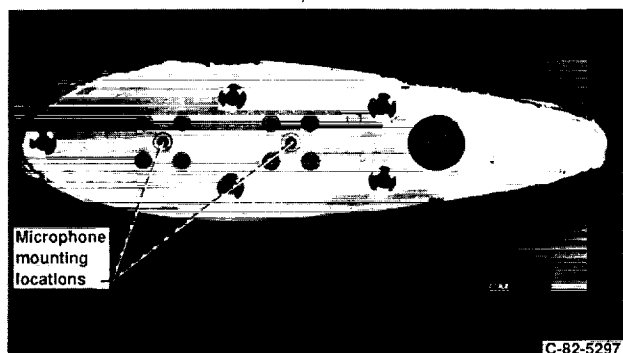


Figure 7.—Wingtip microphone mounting plate.

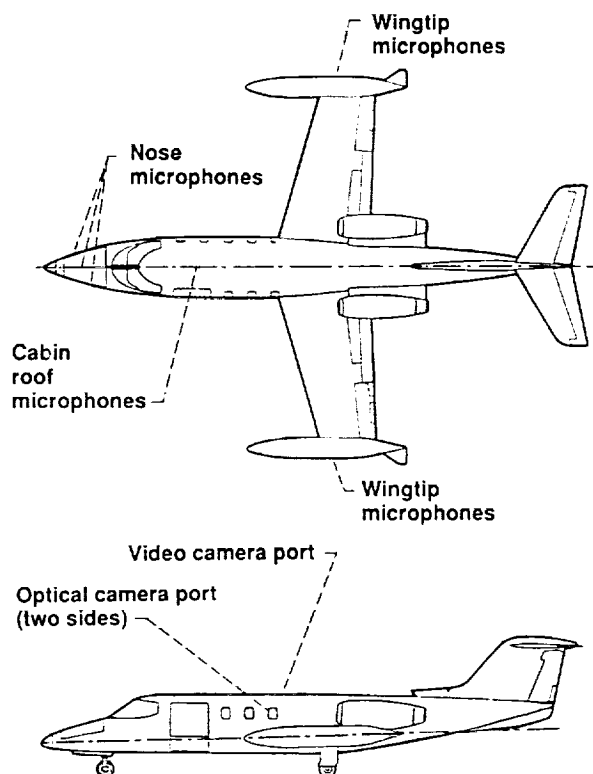
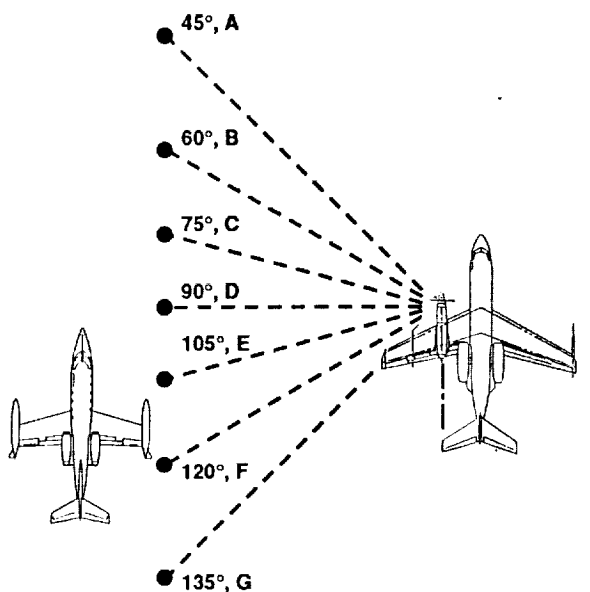
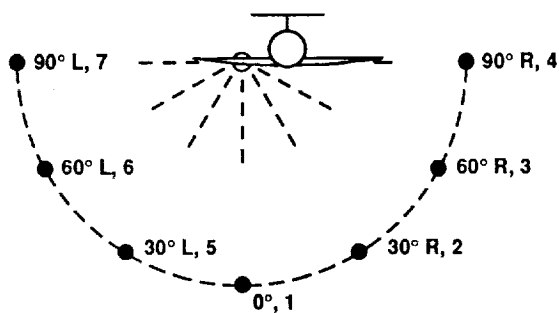


Figure 9.—Learjet acoustic instrumentation.



(a) Sideline angle relative to propeller upstream axis.



(b) Azimuthal angle ( $\phi$ ) viewing upstream.

Figure 10.—Position code for PTA-Learjet station keeping data. Example: position "5E" would nominally be azimuthally 30° left from below the propeller, and at a sideline angle of 105°.

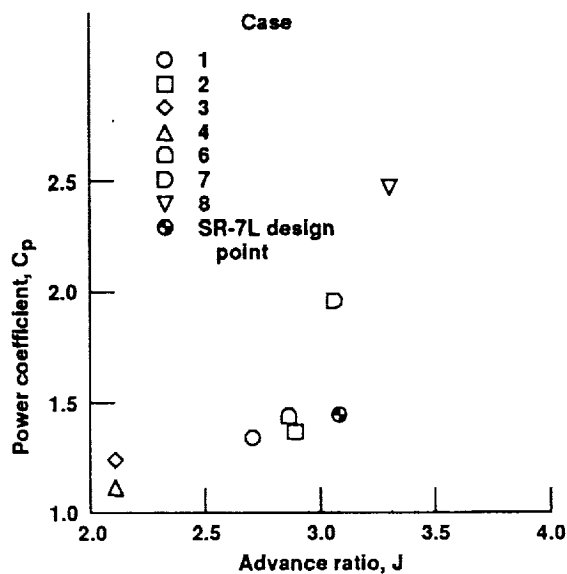


Figure 11.—Propeller operating map.

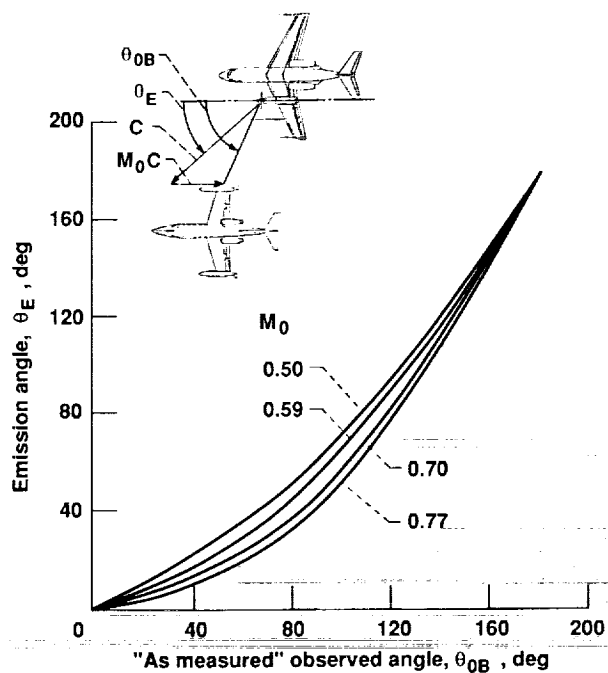


Figure 12.—Relationship between observed and emission angles.  $\theta_E = \theta_{OB} - \sin^{-1}(M_0 \sin \theta_{OB})$



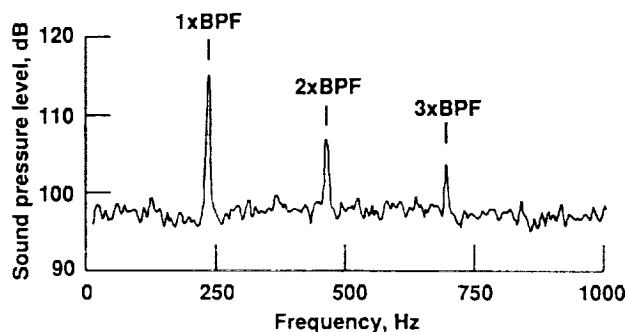


Figure 13.—Representative spectrum of PTA propeller noise. (Measured by Learjet nose microphone, 90°L azimuthal angle, 118° sideline angle, "as-measured" along a 54 m (178 ft) sideline, Case 1 conditions, 4 Hz bandwidth)

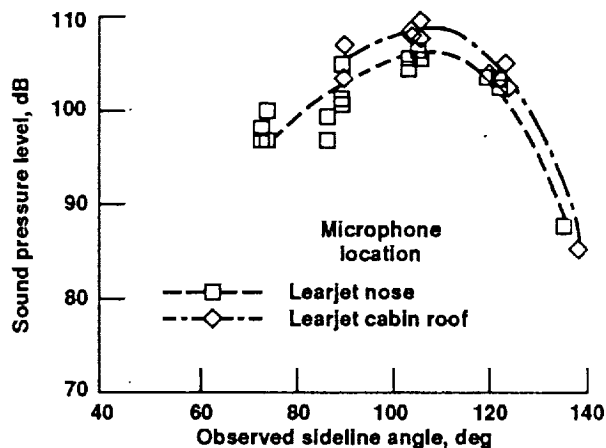


Figure 15.—PTA aircraft sideline directivity, 1xBPF tone, (0° azimuthal location, 0.70 Mach, 10 668 m (35 000 ft) altitude, Case 1 conditions, data adjusted to 152 m (500 ft) free field conditions).

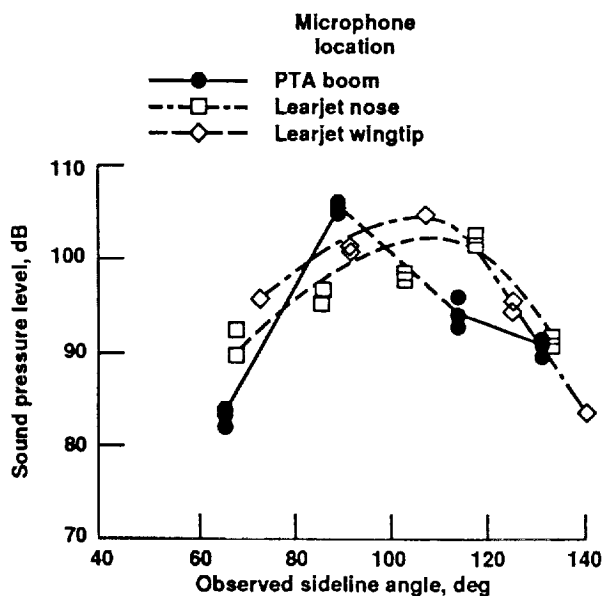


Figure 14.—PTA aircraft sideline directivity, 1xBPF tone, (90°L azimuthal location, 0.70 Mach, 10 668 m (35 000 ft) altitude, Case 1 conditions, data adjusted to 152 m (500 ft) free field conditions).

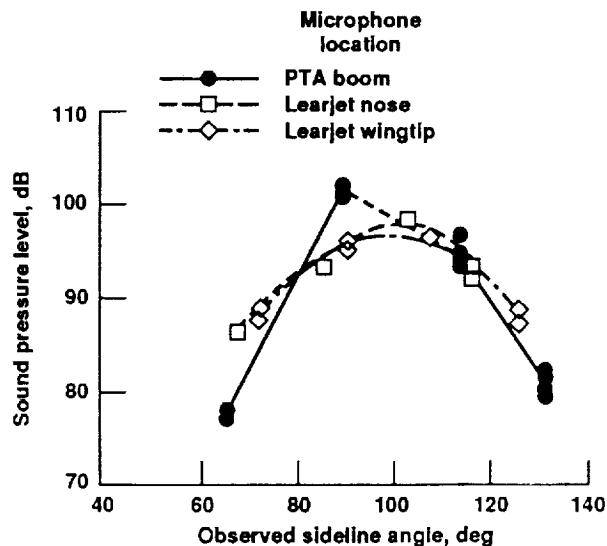


Figure 16.—PTA aircraft sideline directivity, 2xBPF tone, (90°L azimuthal location, 0.70 Mach, 10 668 m (35 000 ft) altitude, Case 1 conditions, data adjusted to 152 m (500 ft) free field conditions).

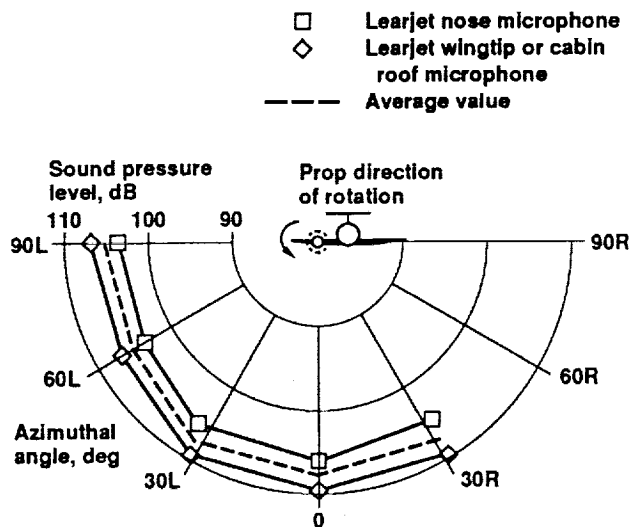


Figure 17.—PTA aircraft azimuthal directivity viewing upstream 1xBPF tone. (0.70 Mach; 10668 M; 35,000 ft altitude; Case 1 conditions. Maximum sideline level, data adjusted to 152 M (500 ft) sideline free field conditions).

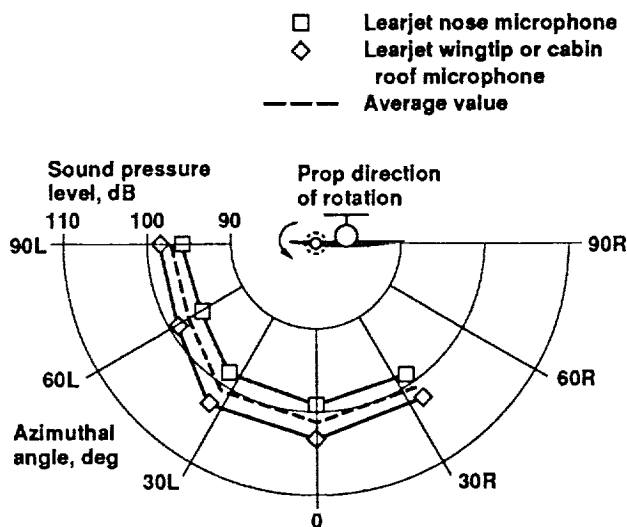


Figure 18.—PTA aircraft azimuthal directivity viewing upstream 2xBPF tone. (0.70 Mach; 10668 M; 35,000 ft altitude; Case 1 conditions. Maximum sideline level, data adjusted to 152 M (500 ft) sideline free field conditions).

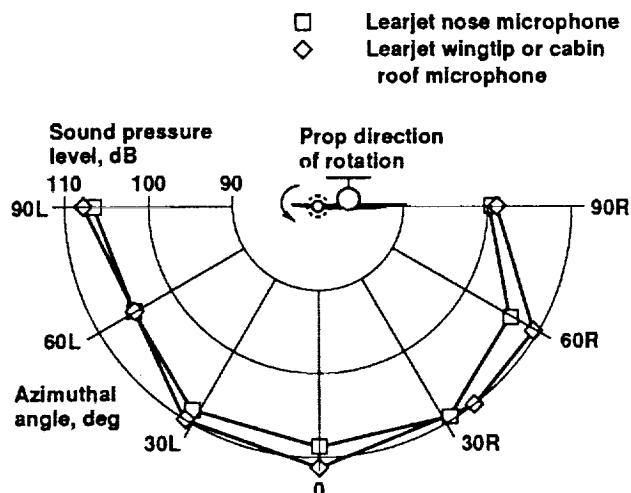


Figure 19.—PTA aircraft azimuthal directivity viewing upstream 1xBPF tone. (0.70 Mach; 6096 M; 20,000 ft altitude; Case 2 conditions. Maximum sideline level, data adjusted to 152 M (500 ft) sideline free field conditions).

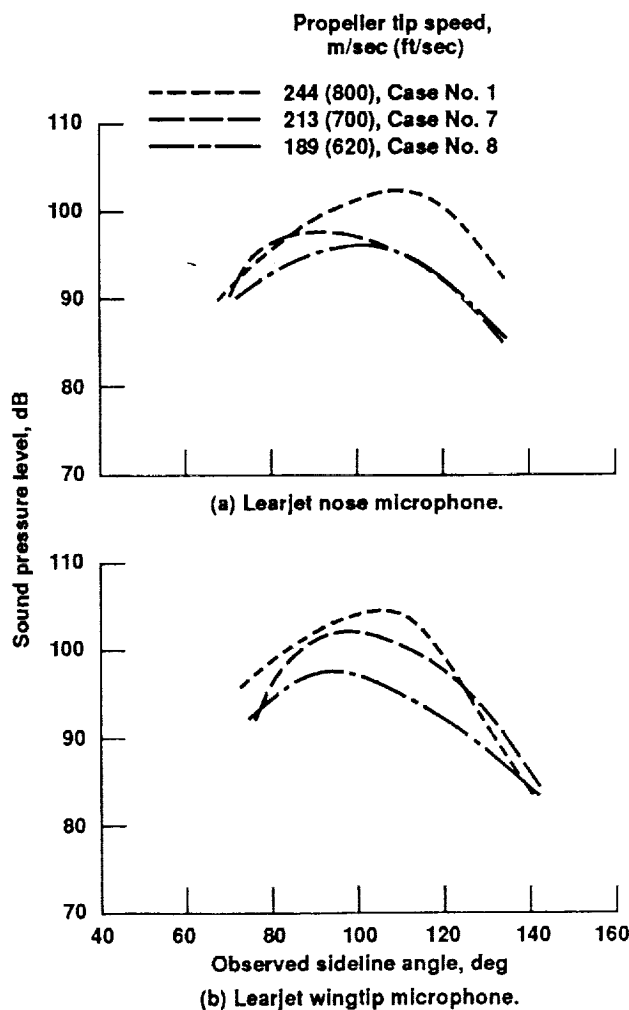


Figure 20.—1xBPF tone sideline directivity, effect of propeller tip speed (0.70 Mach, 10 668 m (35 000 ft) altitude, 90°L azimuthal angle, 152 m (500 ft) sideline.)

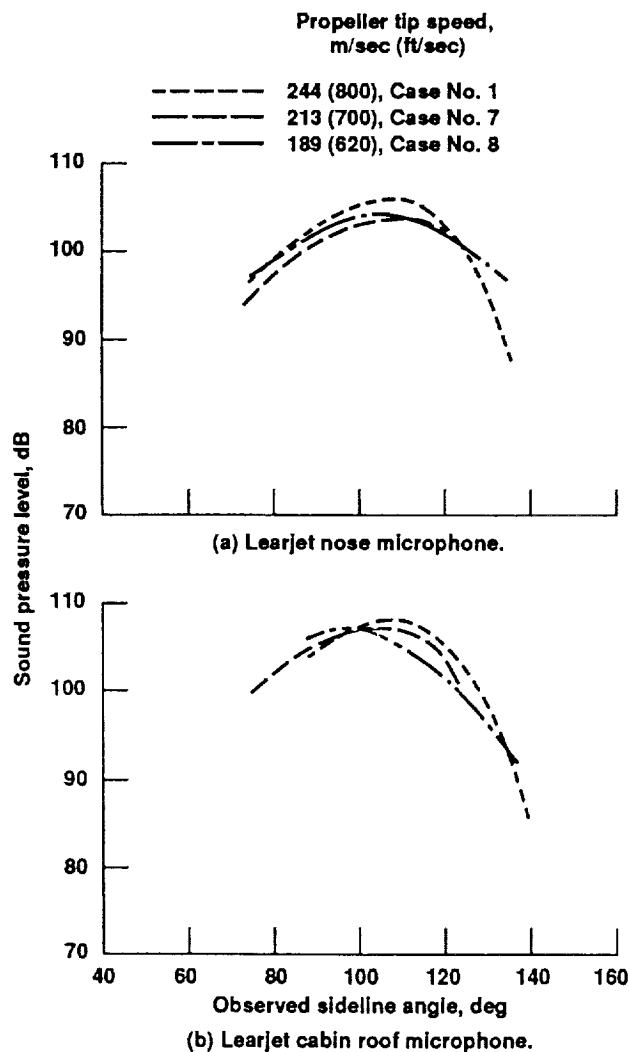


Figure 21.—1x BPF tone sideline directivity, effect of propeller tip speed (0.70 Mach, 10 668 m (35 000 ft) altitude, 0° azimuthal angle, 152 m (500 ft) sideline.)

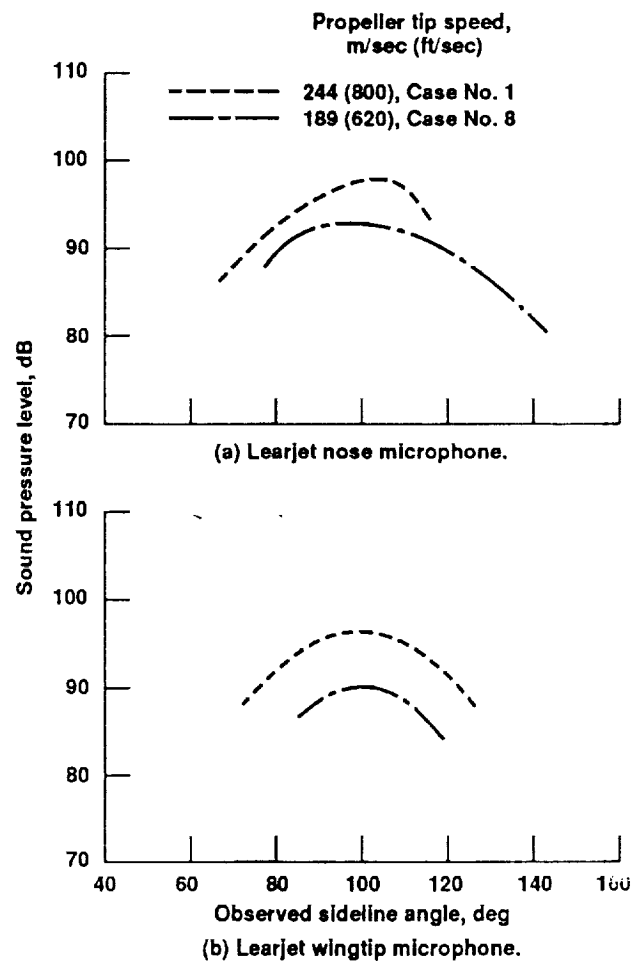


Figure 22.—2x BPF tone sideline directivity, effect of propeller tip speed (0.70 Mach, 10 668 m (35 000 ft) altitude, 90°L azimuthal angle, 152 m (500 ft) sideline.)

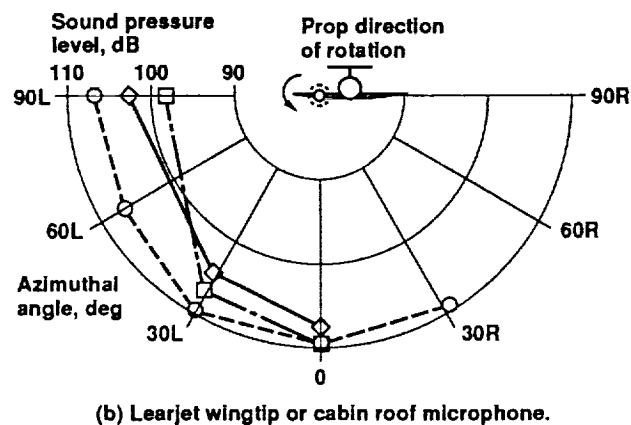
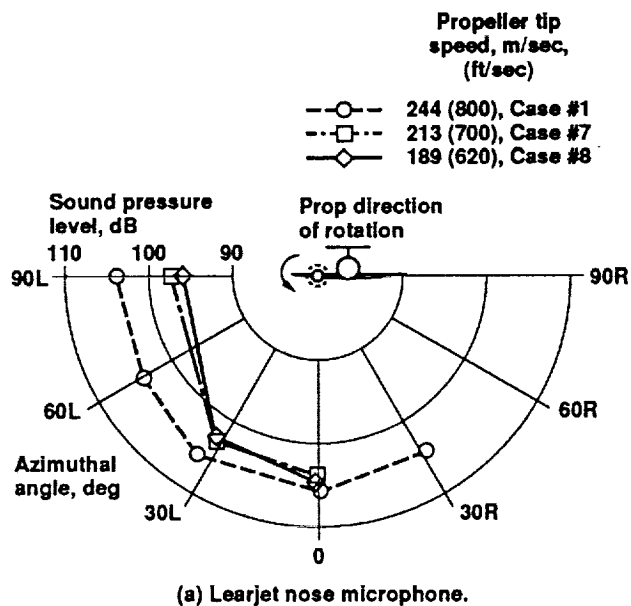


Figure 23.—1x BPF tone azimuthal directivity, effect of propeller tip speed. (0.70 Mach; 10668 M; 35,000 ft altitude; Maximum sideline tone level, 152 M (500 ft) sideline).

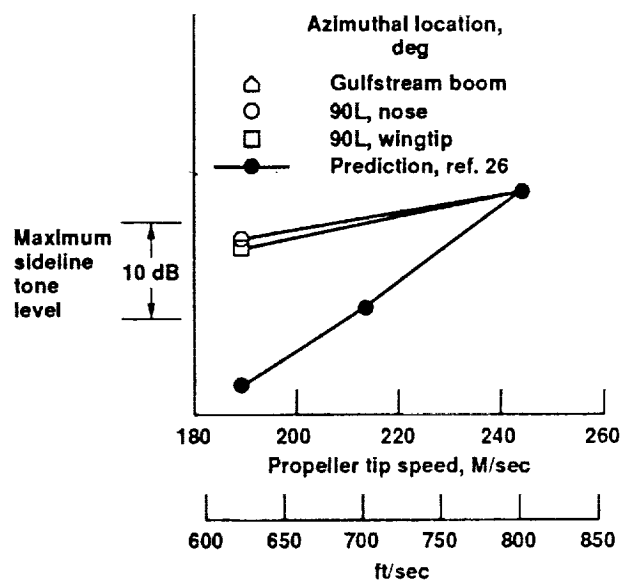
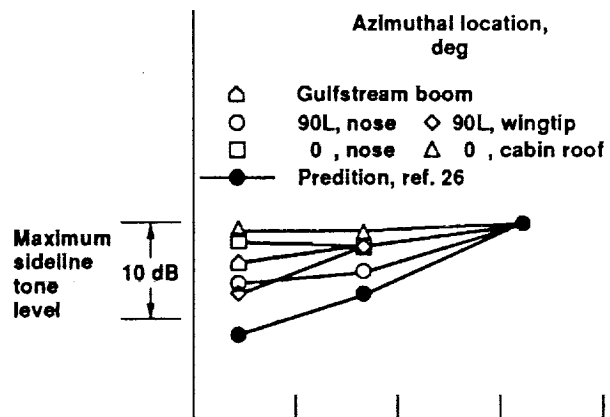


Figure 24.—Effect of propeller tip speed; cases 1, 7, and 8, normalized about 244 M/sec (800 ft/sec) tip speed.

# Report Documentation Page

1. Report No. <b>NASA TM-103687 AIAA-91-0594</b>		2. Government Accession No.		3. Recipient's Catalog No.	
4. Title and Subtitle <b>Inflight Source Noise of an Advanced Full-Scale Single-Rotation Propeller</b>				5. Report Date	
				6. Performing Organization Code	
7. Author(s) <b>Richard P. Woodward and Irvin J. Loeffler</b>				8. Performing Organization Report No. <b>E-5906</b>	
				10. Work Unit No. <b>535-03-01</b>	
9. Performing Organization Name and Address <b>National Aeronautics and Space Administration Lewis Research Center Cleveland, Ohio 44135-3191</b>				11. Contract or Grant No.	
				13. Type of Report and Period Covered <b>Technical Memorandum</b>	
12. Sponsoring Agency Name and Address <b>National Aeronautics and Space Administration Washington, D.C. 20546-0001</b>				14. Sponsoring Agency Code	
15. Supplementary Notes <b>Prepared for the 29th Aerospace Sciences Meeting, sponsored by the American Institute of Aeronautics and Astronautics, Reno, Nevada, January 7-10, 1991. Responsible person, Richard P. Woodward, (216) 433-3923.</b>					
16. Abstract  <b>Flight tests to define the far field tone source at cruise conditions have been completed on the full-scale SR-7L advanced turboprop which was installed on the left wing of a Gulfstream II aircraft. This program, designated Propfan Test Assessment (PTA), involved aeroacoustic testing of the propeller over a range of test conditions. These measurements defined source levels for input into long-distance propagation models to predict en route noise. In-flight data were taken for 7 test cases. The sideline directivities measured by the Learjet showed expected maximum levels near 105° from the propeller upstream axis. However, azimuthal directivities based on the maximum observed sideline tone levels showed highest levels below the aircraft. An investigation of the effect of propeller tip speed (with other engine parameters, such as thrust, shaft power, flight speed, and altitude, held constant) showed that the tone level reduction associated with reductions in propeller tip speed is more significant in the horizontal plane than below the aircraft.</b>					
17. Key Words (Suggested by Author(s)) <b>Noise Advanced turboprop STRL PTA</b>			18. Distribution Statement <b>Unclassified - Unlimited Subject Category 02</b>		
19. Security Classif. (of this report) <b>Unclassified</b>		20. Security Classif. (of this page) <b>Unclassified</b>		21. No. of pages <b>20</b>	
				22. Price* <b>A03</b>	

